CONF-940859--19

EXPERIMENTAL IMPLEMENTATION OF A ROBUST DAMPED-OSCILLATION CONTROL ALGORITHM ON A FULL-SIZED, TWO-DEGREE-OF-FREEDOM, AC INDUCTION MOTOR-DRIVEN CRANE*

Reid L. Kress, J. F. Jansen, and M. W. Noakes
Robotics & Process Systems Division
Oak Ridge National Laboratory
Oak Ridge, TN 37831-6304

To be presented at
ISRAM '94
Fifth International Symposium on Robotics and Manufacturing
Maui, Hawaii
August 14-17, 1994

*Research sponsored by the Office of Technology Development, U.S. Department of Energy, under contract DE-AC05-84OR21400 with Martin Marietta Energy Systems, Inc.

EXPERIMENTAL IMPLEMENTATION OF A ROBUST DAMPED-OSCILLATION CONTROL ALGORITHM ON A FULL-SIZED, TWO-DEGREE-OF-FREEDOM, AC INDUCTION MOTOR-DRIVEN CRANE*

R. L. Kress, J. F. Jansen, and M. W. Noakes
Oak Ridge National Laboratory
Robotics & Process Systems Division
P.O. Box 2008, Building 7601
Oak Ridge, Tennessee 37831-6304

ABSTRACT

When suspended payloads are moved with an overhead crane, pendulum like oscillations are naturally introduced. This presents a problem any time a crane is used, especially when expensive and/or delicate objects are moved, when moving in a cluttered and/or hazardous environment, and when objects are to be placed in tight locations. Damped-oscillation control algorithms have been demonstrated over the past several years for laboratory-scale robotic systems on dc motor-driven overhead cranes. Most overhead cranes presently in use in industry are driven by ac induction motors; consequently, Oak Ridge National Laboratory has implemented damped-oscillation crane control on one of its existing facility ac induction motor-driven overhead cranes. The purpose of this test was to determine feasibility, to work out control and interfacing specifications, and to establish the capability of newly available ac motor control hardware with respect to use in damped-oscillation-controlled systems. Flux vector inverter drives are used to investigate their acceptability for damped-oscillation crane control. The purpose of this paper is to describe the experimental implementation of a control algorithm on a full-sized, two-degree-of-freedom, industrial crane; describe the experimental evaluation of the controller including robustness to payload length changes; explain the results of experiments designed to determine the hardware required for implementation of the control algorithms; and to provide a theoretical description of the controller.

BACKGROUND

One nuclear waste-handling operation examined by the U.S. Department of Energy (DOE), Office of Technology Development (OTD), Robotics Technology Development Program (RTDP), Environmental Restoration and Waste Management (ER&WM) program is transporting heavy objects such as storage casks or barrels from one location to another through cluttered process facility environments. Typically, an object is lifted by a crane hook on the end of a cable, creating a pendulum that is free to swing during transit. This swinging motion makes remote positioning of casks or barrels difficult to control precisely and is potentially

* Research sponsored by the Office of Technology Development, U.S. Department of Energy, under contract DE-AC05-84OR21400 with Martin Marietta Energy Systems, Inc.

destructive to facility equipment and to other storage containers. Typically, a crane operator moves objects slowly to minimize induced swinging and allow time for oscillations to damp out, maintaining safety but greatly decreasing the efficiency of operations. With the control algorithms described herein, even inexperienced operators can move suspended payloads efficiently without large swinging motions.

Damped-oscillation crane control was first implemented on a laboratory-scale test at the Sandia National Laboratories using a CIMCORP XR 6100 gantry robot, a 50-lb weight, and an 80-in. cable [1]. This class of algorithms was further analyzed in Singer and Seering [2], Petterson et al. [3], and Singhose et al. [4]. Oak Ridge National Laboratory (ORNL) implemented the damped-oscillation algorithm on a full-scale crane [5]. These past implementations of damped-oscillation control had two shortcomings: (1) they relied on knowledge of the pendulum characteristics of the suspended payload (model-based control), and (2) they were unable to accept moves that were not completely known in advance. The first shortcoming means that the length of the pendulum must be known prior to motion; however, in real operations, the payload center of gravity and total pendulum length would be difficult to determine a priori, especially within hot cell constraints. The second shortcoming is also detrimental to real operations because most cranes are run by an operator with either remote video viewing or direct line-of-sight viewing. For any practical application, provisions must be made for unknown cable lengths and operator-in-the-loop motion. Both the early Sandia and ORNL systems were computerized dc motor-driven systems and not typical examples of industrial facility cranes. Most industrial cranes (>95%), in particular older DOE hot cell facility cranes, are driven by ac induction motors. Induction motors are inherently more reliable, more likely to be maintenance free, and capable of being designed to be more radiation tolerant than dc motors; therefore, there is considerable incentive to continue to make new facility cranes ac-motor driven. Also, retrofitting existing ac driven facility cranes with new ac drive technology could help minimize remote construction and rewiring operations for facility conversion. Greatly improved commercial variable-speed ac drives (called flux vector drives) are now on the market. These flux vector inverter drives allow the ac induction motor to be controlled over a wide speed range similar to dc servopositioning systems. The applicability of flux vector drive hardware to this control application was demonstrated for 1-degree-of-freedom on an actual industrial crane in Noakes et al. [6]. The primary objectives of the development effort documented in this paper are a description of the experimental implementation of the control algorithm on a full-sized, 2-dof, industrial crane; describe the experimental evaluation of the controller including robustness to payload length changes; explain the results of experiments designed to determine the hardware required for implementation of the control algorithms; and to provide a theoretical description of the controller.

ANALYTICAL DEVELOPMENT

A simple model for a suspended payload system is to consider the system as a rigid-body pendulum, shown in Fig. 1. Assuming that the cable and crane are not flexible, that the center of gravity of the payload is located at L, that there is no damping or other dissipative forces, and that there is motion in only one plane, then the equation governing the physical behavior of the pendulum system can be found in any of several texts (e.g., Higdon et al. [7]; Rao et al. [8]):

$$\ddot{\theta} + \frac{\ddot{x}}{L(t)} \cos\theta + 2\frac{\dot{L}(t)\,\dot{\theta}}{L(t)} + \frac{g}{L(t)} \sin\theta = 0\,, \qquad (1)$$

where all terms are defined in Fig. 1, and the superscript dot represents a derivative with respect to time.

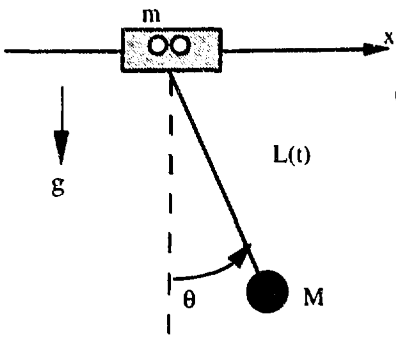

θ = pendulum angle with respect to vertcal (rad)
g = acceleration of gravity (m/s**2)
L(t) = cable length and is a function of time (m)
m = mass of the crane trolley (kg)
M = point mass of the suspended payload (kg)
x = position of pendulum base (m)

Fig. 1. Rigid-bodied pendulum model.

Two approximations will be applied to Eq. (1) based on the physics of the problem. The first is the small angle approximation (i.e., cos $\theta \cong 1$ and sin $\theta \cong \theta$), and the second is that velocities are low enough so that the $\frac{\dot{L}\dot{\theta}}{L}$ term can be ignored. Equation (1) then simplifies to

$$\ddot{\theta} + \frac{g}{L}\theta = -\frac{\ddot{x}}{L} \qquad (2)$$

We wish to use this equation as follows: (1) to develop a formulation to use for controller analysis and (2) to examine the robustness of the system to changes in cable length.

Controller Formulation

To create a formulation useful for controls analysis, consider a system with a pendulum that can move in 2 dof and has damping. State variable form is created, and damping terms ζ_i are included as follows:

$$\frac{d}{dt}\begin{bmatrix} x_0 \\ \dot{x}_0 \\ x_1 \\ \dot{x}_1 \\ \vdots \\ \dot{x}_n \end{bmatrix} = \begin{bmatrix} 0 & 1 & & & & & \\ -\omega_0^2 & -2\zeta_0\omega_0 & & & & & \\ & & 0 & 1 & & & \\ & & -\omega_1^2 & -2\zeta_1\omega_1 & & & \\ & & & & \ddots & & \\ & & & & & -\omega_n^2 & -2\zeta_n\omega_n \end{bmatrix} \begin{bmatrix} x_0 \\ \dot{x}_0 \\ x_1 \\ \dot{x}_1 \\ \vdots \\ \dot{x}_n \end{bmatrix} + \begin{bmatrix} 0 \\ f_1(t) \\ 0 \\ f_2(t) \\ \vdots \\ f_n(t) \end{bmatrix}, \qquad (3)$$

where for the 2-dof application n = 3, or in more compact matrix notation:

$$\dot{\bar{x}} = A\,\bar{x} + \bar{f} \ , \qquad (4)$$

where A refers to the matrix in equation 3.

For the types of problems addressed in this paper, the eigenvalues p_i, for i = 1, 2, ... , 2 (n + 1) associated with Eq. (4) are usually distinct, which means that a complete set of eigenvectors $\bar{v}_i$ can be found such that Eq. (4) can be transformed into the standard uncoupled canonical form,

$$\dot{\bar{z}} = D\,\bar{z} + \bar{u} \, , \qquad (5)$$

where $\bar{x} = M\,\bar{z}$, D = diag (p_i), $\bar{u} = M^{-1}\bar{f}$, M = [$\bar{v}_i$] . The solution to Eq. (5) at time is simply

$$z_i(T) = e^{p_iT} z_i(0) + e^{p_iT} \int_0^T e^{-p_i\tau} u_i(\tau)\, d\tau \quad \text{for } i = 1,2, \ldots, 2n . \tag{6}$$

If we let the input u_i be a time-bounded function (i.e., $u_i(t) = 0$) for time outside of $0 < t < T$, and assuming that all initial conditions are zero, Eq. (6) can be modified to

$$\int_0^\infty e^{-p_i\tau} u_i(\tau)\, d\tau = e^{-p_iT} z_i(T) . \tag{7}$$

The left side of Eq. (7) is the Laplace transform of u_i evaluated at p_i; that is,

$$U_i(s)|_{s = p_i} = \int_0^\infty e^{-p_i\tau} u_i(\tau)\, d\tau = e^{-p_iT} z_i(T) . \tag{8}$$

For the final state $z_i(T)$ to be equal to zero (i.e., no residual vibration), then $U_i(s)|_{s = p}$ must be zero. This means that the Laplace transform of the inputs (f_is) in Eq. (3) must be zero when evaluated at the poles of the dynamic system. This is exactly the condition stated by Bhat and Miu [9], where they proved, even for the case for repeated roots, "that the necessary and sufficient condition for zero residual vibration is that the Laplace transform of the time bounded control input have zero component at the system poles." Furthermore, they mention that, "if the system has non-zero damping, then zero contribution at the system resonant frequency does not guarantee zero residual vibration." This last point is particularly important because in practice the resonant frequencies of a dynamic system are typically known to within a certain precision bound; however, the damping is typically not known, nonlinear by nature, or too troublesome to obtain.

Robust Preshaping

Although they may not be precisely known, the resonant frequencies are usually known to within some tolerance. To avoid residual vibrations, the Laplace transform of the path trajectory must equal zero when evaluated at the poles of the dynamic system. When the poles lie on the $j\omega$ axis, the approach is identical to filtering out the $j\omega$ frequency components of the path trajectory $p(t)$. If the poles do not lie on the $j\omega$ axis and the exact locations of the poles of the dynamic system are unknown, then the standard notch filter will leave some residual vibrations. For this paper, the assumption is made that only the resonant frequencies of the system are known; the damping ratios are unknown and assumed to be zero. To add robustness to the notch filter, the shape of $|P(s)|$, where $P(s) = \mathcal{L}\{p(t)\}$, needs to flatten around the resonant frequencies of the system so as to diminish the residual vibrations (Bhat and Miu [9]). To achieve this flattening, the first n derivatives of $P(s)$ should be equal to zero at the resonant frequencies. As the value of n becomes larger, the system becomes less sensitive to imprecise knowledge of the beam damping and resonant frequencies. This approach, which is formulated in the s domain, has similarities with the time domain approach proposed by Singhose et al. [4], and the interested reader can refer to Murphy and Watanabe [10] for details. From a robustness perspective, it is sufficient to set the first derivative to zero for the crane problem. This is accomplished by setting the zero of the notch filter to have multiplicity of 2. The filter presented is called a robust notch filter (RNF) to highlight its purpose, which is to diminish the impact that imprecise knowledge of the dynamic system poles has on the performance of the filter. The RNF for each resonant frequency is selected as

$$R_n(s) = \frac{\left[\left(\frac{s}{\omega_z}\right)^2 + 1\right]^2}{\left[\left(\frac{s}{\omega_p}\right)^2 + 2\,\frac{\zeta_p}{\omega_p}\,s + 1\right]^2}, \tag{9}$$

where ω_z is the zero resonant frequency, ω_p is the low-pass filter natural frequency, and ζ_p is the damping ratio (set to 1 to achieve a critically damped response). The order of the denominator of Eq. (9) was intentionally set equal to the numerator, which is similar to a conventional notch filter. Although the ω_z term in Eq. (9) is set to the resonant natural frequency of the system, the low-pass filter natural frequency ω_p cannot be selected independently of ω_z. If ω_p is chosen much larger than ω_z, then the numerator term dominates in the frequency range below ω_p, making the numerator essentially a fourth-order differentiator at frequencies from ω_z to ω_p. Any discontinuities in the path, including up to its fourth derivative, could produce large-magnitude oscillations in the system. To avoid this problem, ω_p was set equal to ω_z. Fig. 2 shows a block diagram the implementation of the robust notch filter.

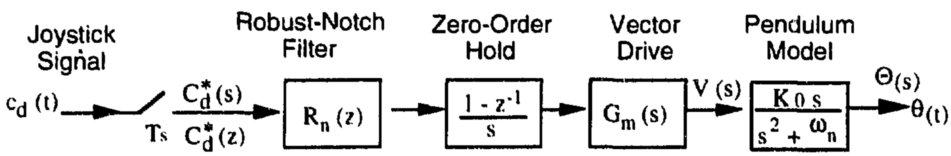

Fig. 2. Open-loop control in velocity mode with joystick.

The robust notch filter is placed in series with a digital zero-order hold preceding the vector drive electronics and is a composite of two notch filters and a lag filter.

Changing Cable Length

To show the effect of changing the cable length, a computer simulation based on the model in Eq. (1) was performed using the following set of parameters: L = 20 [m],

$$\dot{L} = \begin{cases} 0.0625\ [\mathrm{m/s}] & \text{for } t \le 16\ [\mathrm{s}] \\ 0 & \text{for } t > 16\ [\mathrm{s}] \end{cases}, \quad \text{and } \ddot{X} = \begin{cases} 1\ [\mathrm{m/s^2}] & \text{for } t \le 16\ [\mathrm{s}] \\ 0 & \text{for } t > 16\ [\mathrm{s}] \end{cases}.$$

The 16 s break point used for the above parameters was arbitrary, as are both the cable length rate and crane acceleration terms. After 16 s, the cable length will have changed 1 m.

The crane acceleration term is filtered by a second-order notch filter,

$$R_n(s) = \left(\frac{s^2 + \omega_n^2}{s^2 + 2\,\zeta\,\omega_n s + \omega_n^2}\right)^2, \tag{10}$$

where ω_n is the natural frequency of the pendulum ($\sqrt{g/L}$) and ζ is the damping ratio, which is given the values of 1 (it is arbitrary but must be ≥ 1). To demonstrate the robustness of this notch filter, the ω_n term is set to $\sqrt{g/L}$ with L at the initial cable length of 20 m. Plots of the pendulum angle are shown in Figs. 3a and 3b. The filtered acceleration is shown in Fig. 3c. The residual vibration is clearly shown in Fig. 3b, which shows an almost insignificant value of $\approx 0.5 \times 10^{-3}$ rads. which is acceptable. In conclusion, if the crane length is changed slowly and a second-order notch filter is used for the crane acceleration, the residual vibrations can be reduced to an almost insignificant level well within the range of practical application. Larger cable length changes were done on the actual equipment, and these will be discussed in the next section.

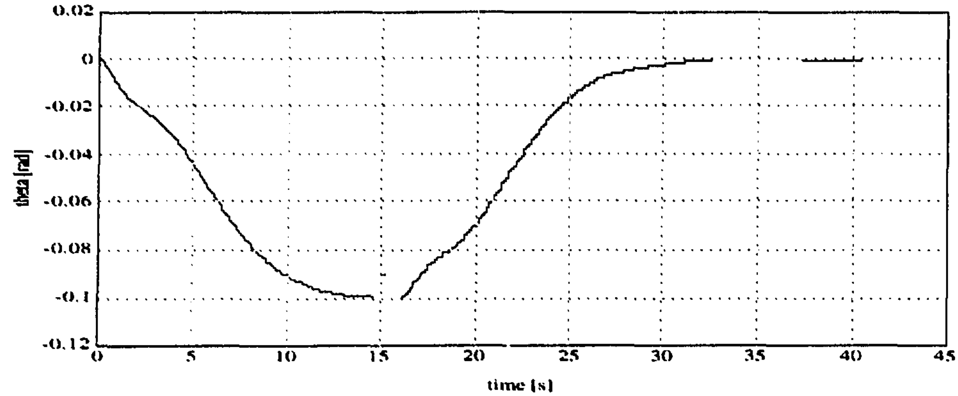

Fig. 3a. Pendulum angle.

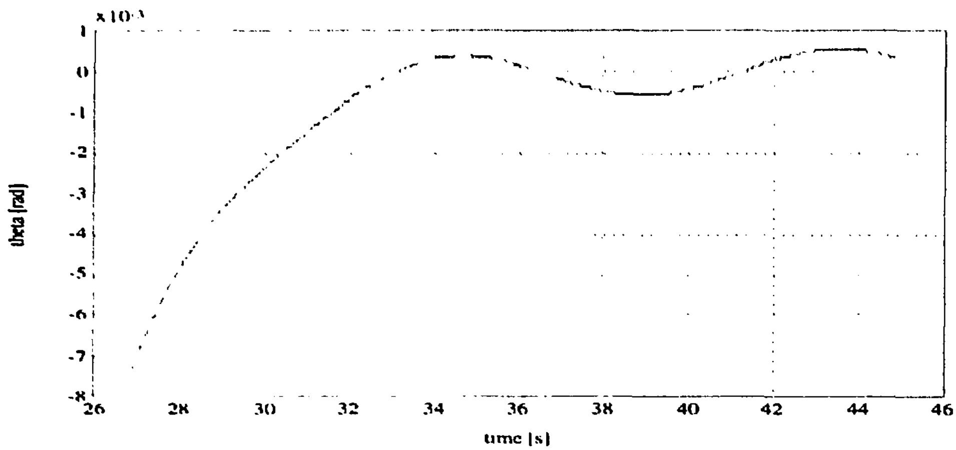

Fig. 3b. Pendulum angle.

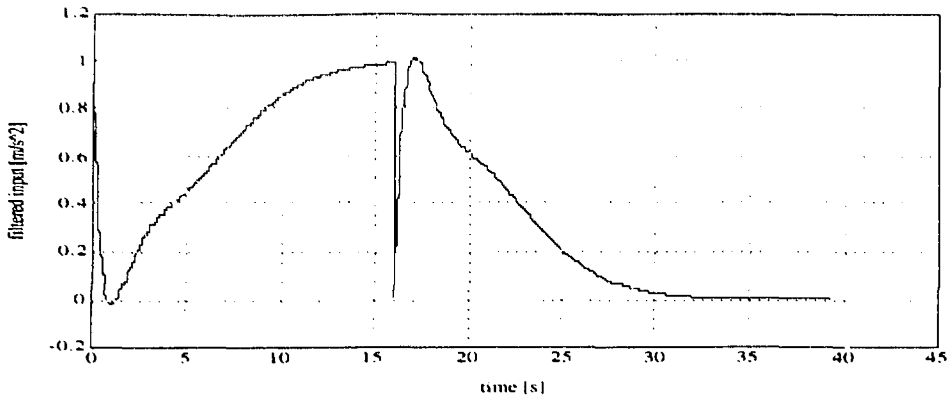

Fig. 3c. Filtered crane acceleration.

EXPERIMENTAL RESULTS

The experimental hardware is the Integrated Process Demonstration (IPD) high-bay overhead crane system, located at ORNL and fitted with a new flux vector inverter drive and motor package for both the bridge and trolley dof, and a computer control system. The IPD crane is a 30-year-old CONCO 25-ton-capacity/3-ton auxiliary crane with all ac motor control. The original ac bridge motor is a 5-hp unit controlled by a switch box. The trolley motor is 3 hp. Drive hardware is a Thor, Inc., three-phase, 480-V ac; a 7.5-hp bridge and a 5.0-hp trolley, flux vector drive with almost 1000:1 speed range capability; and the associated induction motor and rotor encoder. All of the motor control hardware is mounted on the crane trolley, and the computer system is mounted on the bridge. The computer was mounted on the bridge because there was insufficient space on the trolley. A festooning device is used to distribute control signals from the bridge to the trolley-mounted hardware. Initially, a tethered pendant is used for the control interface. The final version will use a radio-frequency (rf) pendant. The crane's original rf pendant remains operable as a safety deadman for the test system.

Computer hardware consists of the Force VME Target 32 backplane and the Force 040 CPU board, which uses a Motorola 68040 processor. The I/O cards include Pentiand MPV906 analog input, MPV922C digital I/O card, and Datel DVME624 analog output cards. The real-time operating system used on the VME rack is VxWorks; the programming languages are C and C++. The development system is a Sun Sparcstation II. Software is developed on the Sun, then target-compiled for the Force 32 VME system, and downloaded via an rf Ethernet link to avoid having to place code in read only memory during the development cycle.

The damped-oscillation controller was first demonstrated using a suspended payload having a natural frequency of 0.135 Hz. The demonstration used an ~14-m-long pendulum, and moves of several meters in 2 dof were attempted. Top speeds of ≈1m/s were obtained. Comparing typical runs with and without the damped-oscillation controller showed residual vibrations being reduced from ±30 cm to ±3 cm (an order of magnitude reduction). Note that this vibration is equivalent to ≈ 2×10^{-3} rads. This is twice what was predicted in Fig. 3b (≈ 1×10^{-3} rads) and is a result of nonlinear friction, imperfect drive wheels and bearing, and measurement inaccuracy present in the real system.

Experiments to determine the speed reduction range necessary for good swing-free control indicate that 10:1 variability is sufficient. The present implementation of the control algorithm can reduce oscillations over large changes in pendulum length. In a typical experiment, the cable length was changed by a factor of four and the residual vibration increased from ±3 cm to ±7 cm. The changes in pendulum length can occur while the other degrees of freedom are moving.

CONCLUSIONS

ORNL has implemented damped-oscillation crane control using a robust notch filter on one of its existing facility ac induction motor-driven overhead cranes. Standard industrial vector drive electronics and a VME-based computer system were used in the implementation. The implementation can be run either robotically (i.e., with a computer generating position commands on a specified path) or teleoperated (i.e., with a human controlling a joystick, as most cranes are presently operated). Tests with this crane and control system showed that residual vibration can be reduced by an order of magnitude and can remain insensitive to large changes in payload location in the vertical direction. The present formulation is computationally undemanding; consequently, future efforts will focus on implementation on smaller, cheaper, and more simple embedded control processors to facilitate future technology transfer to general industry.

REFERENCES

1. Jones, J. F., and Peterson, B. J., "Oscillation Damped Movement of Suspended Objects," pp. 956–962, in *Proceedings of 1988 IEEE International Conference on Robotics and Automation, Philadelphia, PA, April 24-29, 1988.*
2. Singer, N. C., and Seering, W. P., "Design and Comparison of Command Shaping Methods for Controlling Residual Vibration," pp. 888–893, in *Proceedings of 1989 IEEE International Conference on Robotics and Automation, Scottsdale, AZ, May 14-19, 1989.*
3. Peterson, B. J., Robinett, R. D., and Werner, J. C., "Parameter-Scheduled Trajectory Planning for Suppression of Coupled Horizontal and Vertical Vibrations in a Flexible Rod" pp. 916–921, in *Proceedings of 1990 IEEE International Conference on Robotics and Automation, Cincinnati, OH, May 13-18, 1990.*
4. Singhose, W. E., Seering, W. P., and Singer, N. C., "Shaping Inputs to Reduce Vibration: A Vector Diagram Approach," pp. 922–927, in *Proceedings of 1990 IEEE International Conference on Robotics and Automation, Cincinnati, OH, May 13-18, 1990.*
5. Noakes, M. W., Petterson, B. J., and Werner, J. C., "An Application of Oscillation Damped Motion for Suspended Payloads to the Advanced Integrated Maintenance System," *American Nuclear Society Annual Meeting, June 10-14, 1990.*
6. Noakes, M. W., Kress, R. L., and Appleton, G. T., "Implementation of Damped-Oscillation Crane Control for Existing ac Induction Motor-Driven Cranes," *American Nuclear Society Annual Meeting, April 25-30, 1993*, pp. 479–485.
7. Higdon, A., Stiles, W. B., Davis, A. W., and Evces, C. R., *Engineering Mechanics Statics and Dynamics*, Prentice-Hall, 1976.
8. Rao, S. S., *Mechanical Vibrations*, Addison-Wesley, 1990.
9. Bhat, S. P., and Miu, D. K., "Precise Point-to-Point Positioning Control of Flexible Structures," *J. Dyn Syst, Meas, and Control*, 112 (4), 667–674 (December 1990).
10. Murphy, B. R., and Watanabe, I., "Digital Shaping Filters for Reducing Machine Vibration," *IEEE Trans. Robotics and Automation*, 8 (2), 285–89 (April 1992).